Stem Cell Reports
Article

ISSCR

OPEN ACCESS

Expression of α-Smooth Muscle Actin Determines the Fate of Mesenchymal Stromal Cells

Nilesh P. Talele,[1] Julie Fradette,[2] John E. Davies,[3] Andras Kapus,[4] and Boris Hinz[1,*]
[1]Laboratory of Tissue Repair and Regeneration, Matrix Dynamics Group, Faculty of Dentistry, University of Toronto, Toronto, ON M5S 3E2, Canada
[2]Division of Regenerative Medicine, Department of Surgery, Centre de recherche en organogénèse expérimentale de l'Université Laval / LOEX, CHU de Québec Research Centre, Faculty of Medicine, Université Laval, Québec, QC G1J 1Z4, Canada
[3]Institute for Biomaterials and Biomedical Engineering, University of Toronto, Toronto, ON M5S 3G9, Canada
[4]Keenan Research Centre, Li Ka Shing Knowledge Institute, St. Michael's Hospital, and Department of Surgery, University of Toronto, Toronto, ON M5B 1W8, Canada
*Correspondence: boris.hinz@utoronto.ca
http://dx.doi.org/10.1016/j.stemcr.2015.05.004

SUMMARY

Pro-fibrotic microenvironments of scars and tumors characterized by increased stiffness stimulate mesenchymal stromal cells (MSCs) to express α-smooth muscle actin (α-SMA). We investigated whether incorporation of α-SMA into contractile stress fibers regulates human MSC fate. Sorted α-SMA-positive MSCs exhibited high contractile activity, low clonogenicity, and differentiation potential limited to osteogenesis. Knockdown of α-SMA was sufficient to restore clonogenicity and adipogenesis in MSCs. Conversely, α-SMA overexpression induced YAP translocation to the nucleus and reduced the high clonogenicity and adipogenic potential of α-SMA-negative MSCs. Inhibition of YAP rescued the decreased adipogenic differentiation potential induced by α-SMA, establishing a mechanistic link between matrix stiffness, α-SMA, YAP, and MSC differentiation. Consistent with in vitro findings, nuclear localization of YAP was positively correlated in α-SMA expressing stromal cells of adiposarcoma and osteosarcoma. We propose that α-SMA mediated contraction plays a critical role in mechanically regulating MSC fate by controlling YAP/TAZ activation.

INTRODUCTION

Human mesenchymal stromal cells (MSCs) are being used in cell therapy to support organ regeneration after injury, e.g., by injection into the heart after myocardial infarction (Behfar et al., 2014). However, the outcomes of MSC therapy have been variable and the reasons for success or failure are a matter of ongoing debate (Behfar et al., 2014; Bianco et al., 2013). First, the potential of MSC therapy to support organ regeneration depends on the intrinsic character of the transplanted cell population, which is often ill-defined (Bianco et al., 2013; Mishra et al., 2009; Prockop et al., 2014). Second, engraftment success, survival, phenotype, and activity of MSCs strongly depend on the microenvironment present at the site of delivery (Forbes and Rosenthal, 2014). This microenvironment often shares features of a healing wound, including inflammatory cells, neo-vasculature, and pro-fibrotic cytokines such as TGF-β1 (Forbes and Rosenthal, 2014). Tissue repair and tumor microenvironment can convert MSCs into contractile myofibroblasts (MFs) that de novo form α-smooth muscle actin (α-SMA)-containing stress fibers (Hinz, 2010a; Hinz et al., 2012). The most prominent examples are "cancer-associated fibroblasts" (CAFs) which originate at least in part from bone marrow-derived MSCs (Karnoub et al., 2007; Mishra et al., 2009; Öhlund et al., 2014; Quante et al., 2011).

Acute and transient MF activation is part of the body's normal wound healing program, but persistent MFs contribute to fibrosis by excessively producing and contracting collagenous extracellular matrix (ECM) into stiff scar tissue (Hinz et al., 2012). In turn, the stiffness of mature scar promotes mechanical activation of MFs (Hinz, 2010b). In cell therapy, MSCs engrafted into early stages of organ fibrosis were shown to improve healing, but delivery into stiff mature scar further enhanced fibrogenesis in fibrotic lung, kidney, liver, and heart (Breitbach et al., 2007; di Bonzo et al., 2008; Nagaya et al., 2005; Ninichuk et al., 2006; Yan et al., 2007). Substrate mechanics in conjunction with intracellular tension have also been shown to determine the preference of naive MSCs toward specific lineages (Engler et al., 2006; Winer et al., 2009; Yang et al., 2011, 2014), but the functional consequences of MF activation (fibrogenesis) on MSC clonogenicity and lineage differentiation potential have not been systematically investigated.

We hypothesize that acquisition of MF contractile features, most notably expression of α-SMA, will determine the fate of bone-marrow-derived human MSCs (hMSCs). Our results show that α-SMA-positive hMSCs exhibit low self-renewal and lineage differentiation potential, in contrast to α-SMA-negative hMSCs, which are clonal and multi-potent. Soft culture substrates that suppress the pro-fibrotic MF phenotype also enhance the lineage differentiation potential of α-SMA-positive hMSCs. We identify

α-SMA incorporation into hMSC stress fibers and downstream translocation of YAP/TAZ transcription factors into the nucleus as a key event in regulating genes associated with self-renewal and differentiation. Inhibition of α-SMA may thus be a potential strategy to improve the therapeutic potential of MSCs and reduce the risk of MSC fibrogenesis.

RESULTS

MF Activation Results in Reduced Clonogenicity and Differentiation Potential of hMSCs

Independently of MSC origin, MF activation occurs spontaneously in standard cell culture on rigid tissue culture plastic in serum-containing media. Cultured hMSCs derived from adipose tissue, umbilical cord perivasculature, and bone marrow all developed MF characteristics, including α-SMA-positive stress fibers, extradomain-A fibronectin (ED-A FN) in the ECM, and high contractile activity, which were enhanced by TGF-β1 (Figure S1). To test whether MF activation affected stem cell features, we focused on bone-marrow derived hMSCs (Figure 1A). In standard culture, 17% ± 4.2% of hMSCs expressed α-SMA in F-actin-positive stress fibers, which increased to 32% ± 5.1% after TGF-β1 treatment, associating with 3.5-fold higher contraction (Figures 1A, 1B, and S1). TGF-β1 treatment reduced the number of colony forming units-fibroblasts (CFU-F) by 3-fold (Figure 1B) and the ability of hMSCs to differentiate into adipogenic (10-fold) and osteogenic (7-fold) cell lineages in conventional lineage-induction assays supplemented with TGF-β1 (Figure 1B). TGF-β1 treatment resulted in ~1.5-fold increase in median fluorescence intensity of common MSC markers such as CD44, CD73, and CD90, but did not change levels of CD105 and CD166 (Figure S2). This supports the onset of a fibrogenic program since CD44, CD73, and CD90 have all been identified on fibroblasts and are upregulated in conditions of fibrosis (Fernández et al., 2013; Koumas et al., 2003; Li et al., 2011; Maring et al., 2012; McQualter et al., 2013).

To test whether low ECM stiffness, a powerful inhibitor of MF activation (Goffin et al., 2006), improves hMSC clonogenicity and lineage differentiation potential, we cultured hMSCs on silicone substrates with different Young's elastic modulus simulating different scar maturation stages (Figure 1C). Expression of α-SMA and ED-A FN decreased after 5 days culture on "fibrosis-rigid" (65 kPa) over "wound-stiff" (26 kPa) to "normal tissue-soft" (3 kPa) substrates (Figures 1D and 1E). With percentages of α-SMA stress fiber-positive hMSCs decreasing from 21.9% ± 3.4% (65 kPa) to 17.3% ± 2.4% (26 kPa) and 5.7% ± 3.1% (3 kPa) (Figure 1F), the number of CFU-F increased (Figure 1G). Treatment with TGF-β1 enhanced α-SMA expression on 26 kPa and 65 kPa substrates compared to non-treated controls, but also reduced CFU-F capacity independently of α-SMA content (3 kPa). This finding is consistent with previous studies reporting inhibitory effects of TGF-β1 on mesenchymal cell proliferation (Kim et al., 2014) and MSC self-renewal capacity by inducing osteogenesis and chondrogenesis (Watabe and Miyazono, 2009). Consistently, our hMSCs exhibited ~8-fold increase in the early chondrogenic marker *SOX9* and ~50-fold increase of the late marker *ACAN* (aggrecan) upon TGF-β1stimulation. Whereas *ACTA2* was also increased by TGF-β1 treatment in conventional culture conditions (~8-fold), expression levels remained low in complete chondrogenesis medium (containing TGF-β) and pellet culture that induced *SOX9* (~7-fold) and substantially *ACAN* (~180-fold) (Figure S1). Hence, using TGF-β1 as a stimulus is not suitable to test whether MF activation is directing hMSC stem cell potential.

α-SMA-Positive hMSCs Exhibit Low Clonogenicity and Bias toward Osteogenic Potential

To answer whether loss of hMSC stem cell features on stiff substrates is a consequence of MF activation and α-SMA expression, we sorted α-SMA-positive and α-SMA-negative hMSC from heterogeneous hMSC using flow cytometry (Figure 2A). Because no cell surface marker reliably identifies MFs, we sorted based on the observation that α-SMA-expressing hMSCs exhibited about six times larger spreading area than α-SMA-negative cells (Figure 2A). After live-sorting the lower and higher quartile of hMSCs by size, the large-size-sorted fraction contained no α-SMA-negative cells, whereas only 2.3% of the small-sorted population were α-SMA-positive (Figure 2B). For the remainder of this study, size-sorted hMSCs were thus termed SMA(−) (small) and SMA(+) (large). The pro-fibrotic character of SMA(+) hMSCs extended beyond expression of α-SMA as shown by higher mRNA levels of pro-fibrotic markers *ACTA2*, COL1A1, COL3A1, CTGF, and TGFB2 as compared to SMA(−) hMSCs (Figure 2C).

SMA(−) hMSCs contained 8-fold more CFU-Fs compared with SMA(+) hMSCs (Figure 2D) and in single cell cloning assays, formed ~8-fold more clones than unsorted hMSCs; SMA(+) hMSCs did not produce any clones (Figure 2D). Consistently, mRNA levels of *SOX2*, *OCT4*, and *DNMT1* genes that are indicative and instrumental for stem cell self-renewal and clonogenicity in MSCs (Arnold et al., 2011; Tsai et al., 2012; Yannarelli et al., 2013; Yu et al., 2012b), were ~5-fold lower in SMA(+) compared with SMA(−) hMSCs (Figure 2E). When cultured under respective lineage induction conditions, SMA(−) hMSCs

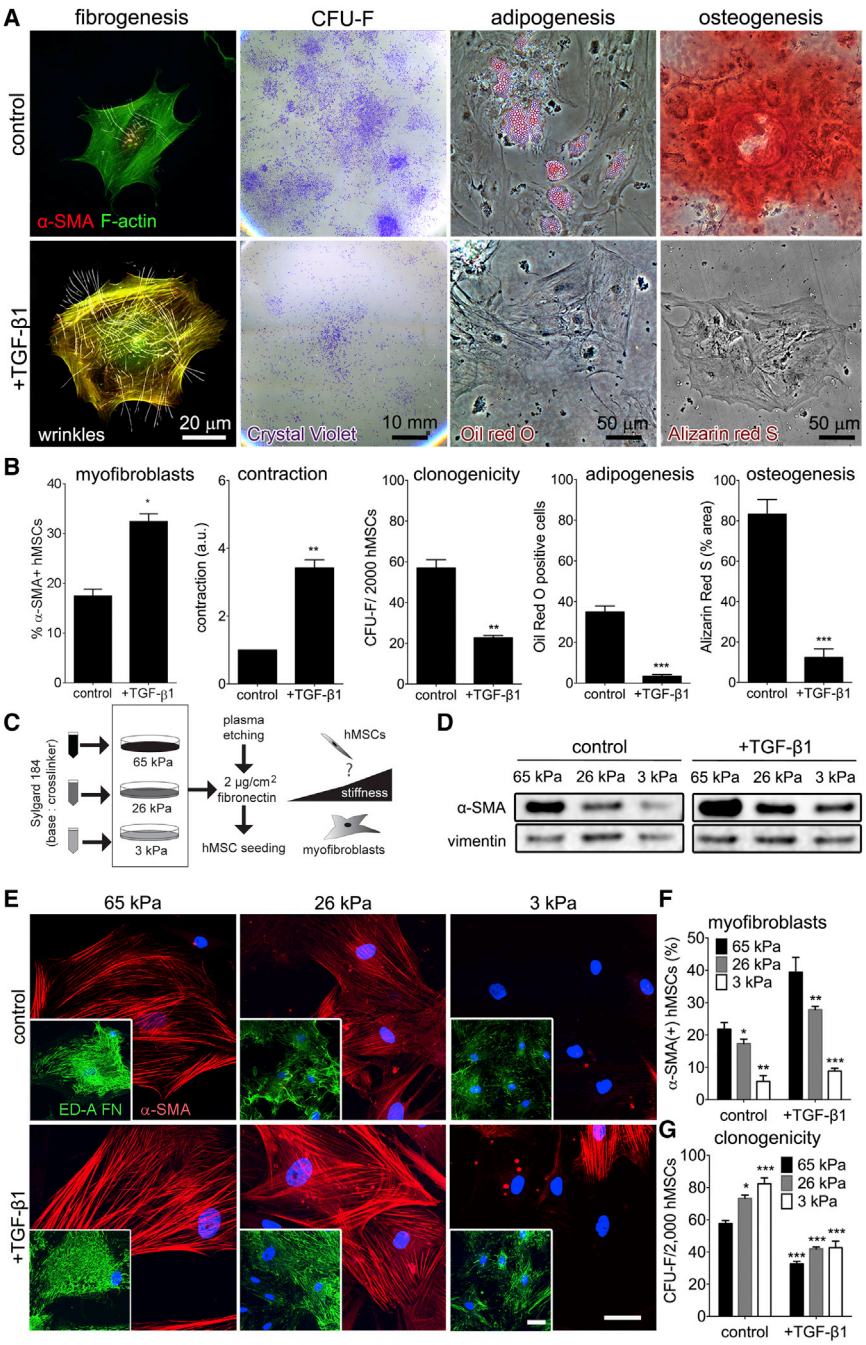

Figure 1. hMSC-to-MF Activation Reduces Clonogenicity and Lineage Differentiation Potential

(A and B) hMSCs were cultured with and without TGF-β1 (2 ng/ml) for 4 days to assess MF activation by staining for α-SMA (red) and stress fibers (F-actin, green), for 10 days to assess CFU-F formation, and 14 days to assess adipogenesis (oil-red-O-positive lipids) and osteogenesis (Alizarin Red S-positive mineralized nodules) in respective induction media (+TGF-β1). (B) MF activation was quantified by assessing the percentage of α-SMA expressing hMSCs. The contraction was assessed by growing hMSC on deformable wrinkling substrates (white lines in immunofluorescence image overlay) and quantifying the total wrinkle area normalized by cell numbers. Clonogenicity was assessed by counting the number of colonies formed after 10 days.

(C–G) HMSCs were cultured on FN-coated silicone substrates, mimicking fibrosis-rigid (65 kPa), wound-stiff (26 kPa), and normal-tissue-soft (3 kPa) environments. (D) After 5 days, cells were analyzed by western blotting for α-SMA and vimentin (loading control) and (E) immunofluorescence for α-SMA (red) and ED-A FN (green). The scale bar represents 50 μm. (F) MF activation was quantified as percentage of α-SMA stress fiber positive cells. (G) Clonogenicity was quantified in CFU-F assays on differently stiff substrates.

All of the graphs show averages ± SD from at least five independent experiments (*$p \leq 0.05$, **$p \leq 0.005$, and ***$p \leq 0.0005$ using ANOVA followed by a post hoc Tukey's multiple comparison test). See also Figure S1.

differentiated into both lipid-producing and *PPARG* transcript expressing adipocytes and osteoblasts that expressed *RUNX2* and formed mineralized nodules (Figure 2F). In contrast, SMA(+) hMSCs exhibited substantially reduced adipogenic potential, but enhanced osteogenesis (~4- fold more mineralized nodules) (Figure 2F). Collectively, these results indicate that the α-SMA-positive fraction of hMSC populations is fibrogenic, non-clonal, and biased toward osteogenesis.

Mechanical Deactivation Restores the Differentiation Potential of SMA(+) hMSCs

We next addressed whether expression of α-SMA in hMSCs hallmarks reversible MF activation or terminal fibrogenic differentiation by culturing pure SMA(+) hMSCs for 5 days on soft culture substrates. α-SMA protein levels and sizes of cell-ECM focal adhesions decreased with decreasing substrate stiffness (Figure S3). Cell culture on 3 kPa soft substrates resulted in 2-fold reduced expression

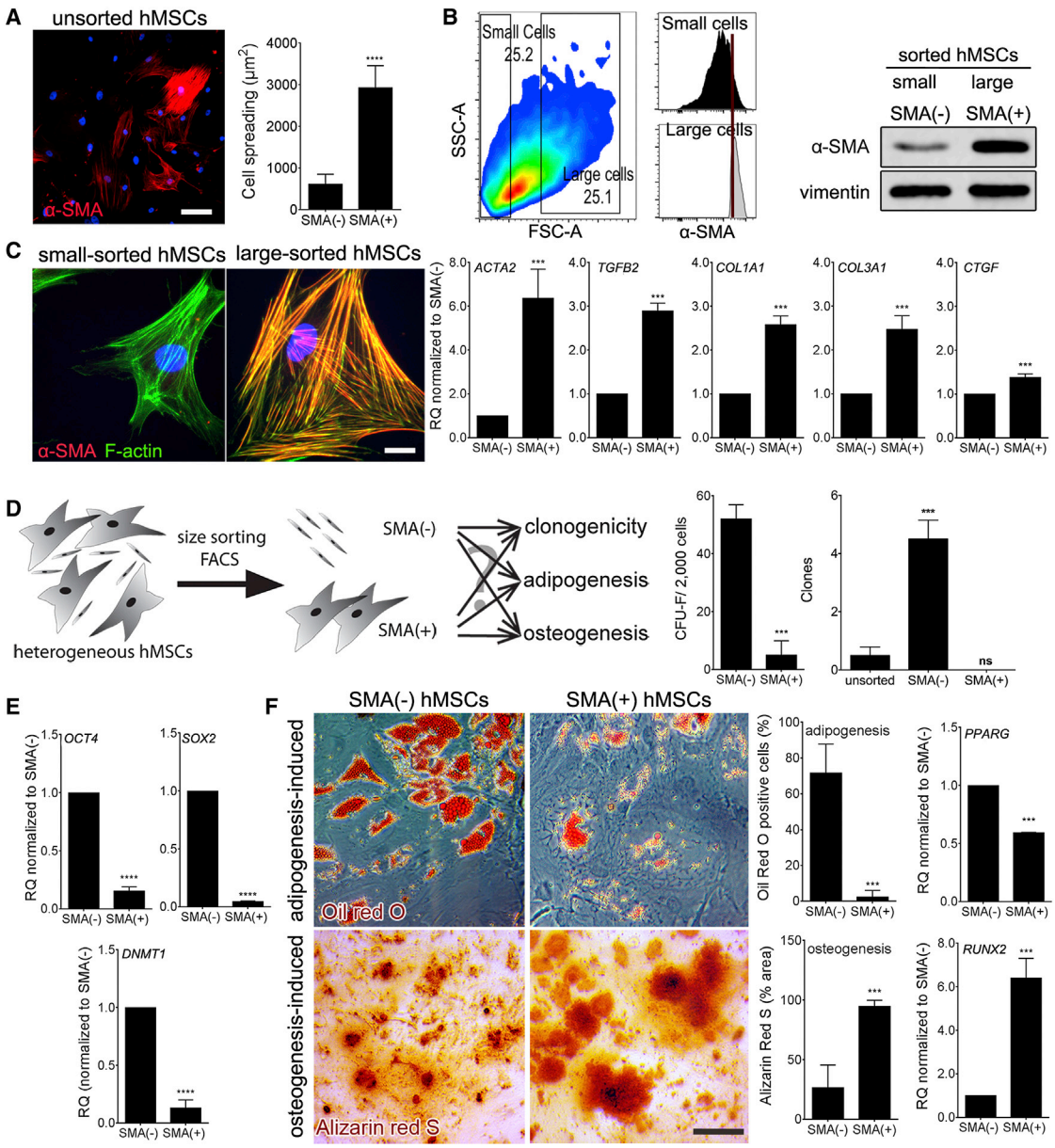

Figure 2. Clonal and Differentiation Potentials Are Higher in Enriched α-SMA-Negative Than in α-SMA-Positive hMSC Populations

(A) hMSCs spontaneously acquire the MF phenotype, resulting in a heterogeneous population of α-SMA-positive (red) and -negative cells (nuclei only, blue). The scale bar represents 50 μm. The cell spreading area was measured as a function of α-SMA expression.

(B) Heterogeneous hMSC populations were sorted into small (lower 25%) and large hMSCs (upper 25%) using forward scatter in FACS and then immunostained for α-SMA in suspension or analyzed by western blotting.

(C) Small size-sorted hMSC, now defined as "SMA(−)" and large-size sorted "SMA(+)" hMSCs, were cultured for 1 day on stiff substrates to assess α-SMA (red) and stress fibers (F-actin, green). Transcript levels were quantified for pro-fibrotic markers *ACTA2* (α-SMA), TGFB2 (TGF-β2), COL1A1 (collagen type I), COL3A1 (collagen type III), and CTGF (CCN2) using quantitative (q)RT-PCR.

(D and E) Sorted SMA(−) and SMA(+) hMSCs were assessed for clonogenicity in functional CFU-F and single cell cloning assays and assessed for (E) levels of self-renewal markers *OCT4*, *SOX2*, and *DNMT1*.

(F) Sorted SMA(−) and SMA(+) hMSCs were lineage-induced in adipogenic and osteogenic induction medium and assessed for adipogenesis using oil red O staining and qRT-PCR analysis for *PPARG* and osteogenesis using Alizarin Red S staining and qRT-PCR analysis for *RUNX2*. The scale bars represent (A) 50 μm and (C and F) 50 μm. The graphs show averages ± SD from at least five independent experiments (*$p \leq 0.05$, **$p \leq 0.005$, and ***$p \leq 0.0005$ using Student's t test). See also Figure S2.

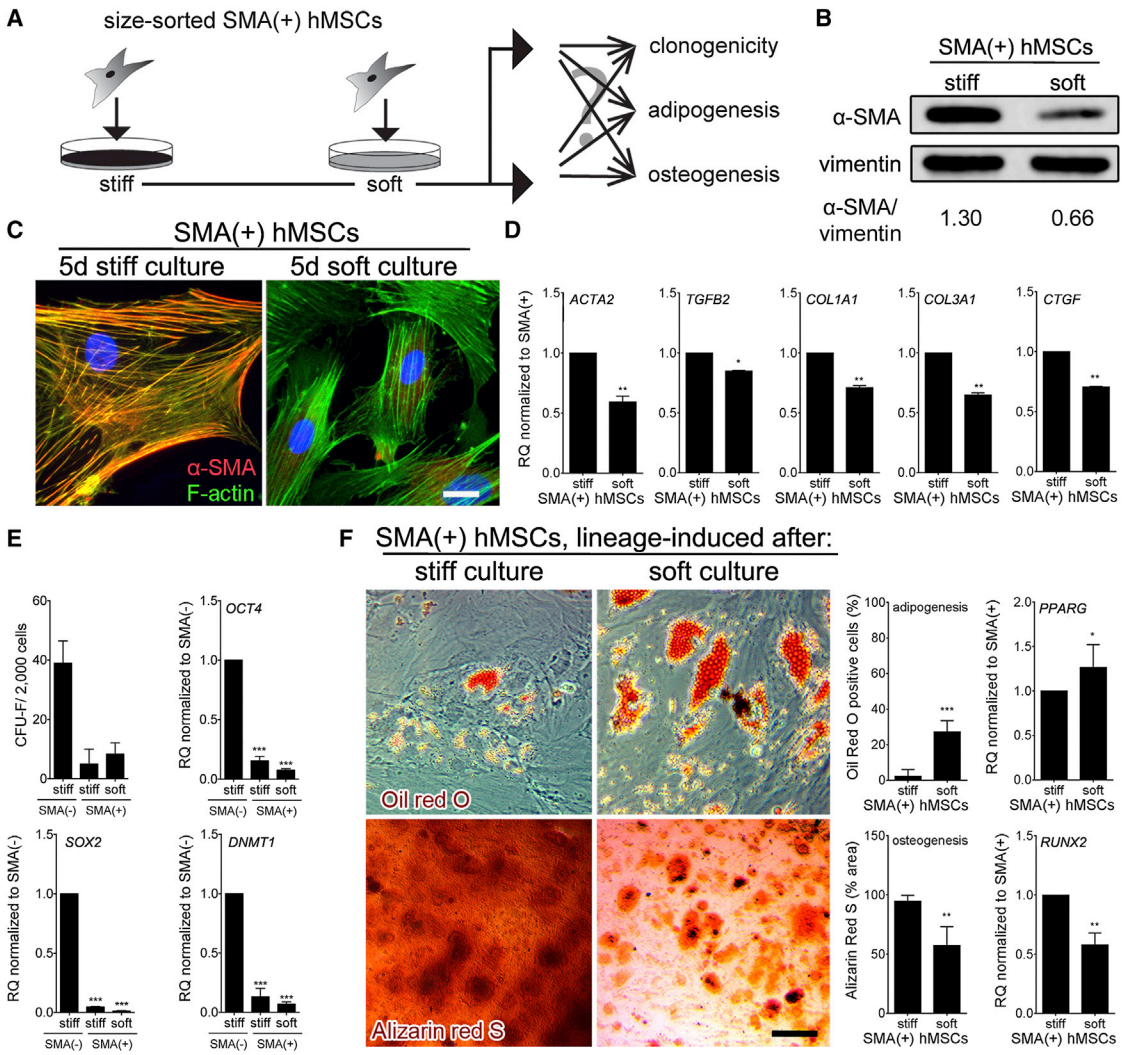

Figure 3. Soft Substrate Culture Restores Lineage Differentiation of SMA(+) hMSCs

(A–D) Sorted SMA(+) hMSCs were cultured on stiff and soft substrates and assessed for MF activation after 5 days, clonogenicity after 10 days, and differentiation potential after 14 days. MF activation was assessed by (B) western blotting, (C) immunofluorescence for α-SMA (red) and stress fibers (F-actin, green) (the scale bar represents 20 μm), and (D) qRT-PCR for fibrotic markers.

(E) Self-renewal potential was quantified from CFU-F assays and qRT-PCR analysis of *OCT4*, *SOX2*, and *DNMT1* transcripts.

(F) Sorted SMA(+) were grown for 5 days on stiff and soft culture substrates and then transferred to conventional culture dishes for induction into adipogenic lineage (oil red O, *PPARG*) and osteogenesis (Alizarin Red S, *RUNX2*). The scale bar represents 50 μm.

The graphs show averages ± SD from at least five independent experiments (*$p \leq 0.05$, **$p \leq 0.005$, and ***$p \leq 0.0005$ using Student's t test). See also Figure S3.

of α-SMA (Figures 3A and 3B), disappearance of α-SMA from stress fibers (Figure 3C), and generally reduced levels of fibrotic marker transcripts compared with hMSC(+) grown on stiff substrates (Figure 3D). The culture time required to deactivate MFs mechanically was 5 days (Figure S4). Reversibility of the fibrotic phenotype was not dependent on the degree of MF pre-activation. SMA(+) hMSCs lost the MF phenotype on soft substrate even when being sorted from TGF-β1-pre-treated heterogeneous populations and were not re-activated on soft substrate by adding TGF-β1 (Figure S4).

Transfer of SMA(+) hMSCs that had lost MF characteristics on soft substrates to conventional lineage induction media resulted in 1.3-fold higher levels of *PPARG* mRNA and ~10-fold increase in lipid-production than SMA(+) hMSCs harvested from control stiff culture (Figure 3E). Conversely, the osteogenic capacity of soft-grown SMA(+) hMSCs was reduced by ~2-fold compared

to SMA(+) hMSCs from stiff cultures (Figure 3E). However, clonogenicity and mRNA levels of *OCT4*, *SOX2*, and *DNMT1* of "MF-deactivated" SMA(+) hMSCs were similarly low compared with control SMA(+) hMSCs grown on stiff substrates (Figure 3F). Hence, SMA(+) hMSC can be deactivated to lose fibrotic MF features by reducing substrate stiffness, but do not regain clonogenicity, possibly due to a dose-dependent effect of substrate stiffness on MF (de)activation. To achieve greater changes in MF activation state and to test whether the MF marker α-SMA plays a functional role in guiding MSC fate, we next overexpressed and knocked down α-SMA in MF-sorted hMSC populations.

Expression of α-SMA Directly Controls hMSC Fate

Expression of α-SMA and incorporation into stress fibers upregulate contraction of fibroblastic cells (Hinz et al., 2001, 2002). It is conceivable that α-SMA directly regulates hMSC stem cell character because actin-myosin generated intracellular tension guides hMSC fate decision (Engler et al., 2006; MacQueen et al., 2013; McBeath et al., 2004; Swift et al., 2013). To elucidate the role of α-SMA protein in directing hMSC fate, we first transfected SMA(−) hMSCs with α-SMA-GFP (Figure 4A) that localized to stress fibers and GFP control that remained cytosolic (Figure 4B). Expression of SMA-GFP (67 kDa) resulted in upregulation of endogenous α-SMA (42 kDa) (Figure 4B), consistent with a positive feedback loop of enhanced cell contraction and mechanically induced α-SMA expression (Hinz et al., 2002). Overexpression of α-SMA-GFP reduced the high clonogenicity of SMA(−) hMSCs and transcript levels of *SOX2*, *OCT4*, and *DNMT1* by maximally 4-fold compared to GFP control (Figure 4C). α-SMA-GFP-overexpressing SMA(−) hMSCs exhibited ∼5-fold decreased adipogenesis (Figure 4D), but ∼2-fold increased osteogenic potential compared to controls (Figure 4D).

Next, we knocked down α-SMA in SMA(+) hMSCs using short hairpin (sh)RNA directed against α-SMA, which resulted in ∼3-fold higher numbers of CFU-Fs and dramatic upregulation of *SOX2*, *OCT4*, and *DNMT1* transcripts (up to 40-fold, *OCT4*) than in controls (scrambled shRNA with GFP reporter) (Figure 4G). In cell lineage induction assays, SMA(+) hMSCs showed ∼25-fold increased formation of lipid-producing adipocytes, ∼5.6-fold higher *PPARG* mRNA levels (Figure 4H), and ∼2.2-fold decrease of mineralized nodule area, as well as ∼100-fold decrease in *RUNX2* mRNA levels after α-SMA knockdown compared with controls (Figure 4H). Our results showing that knockdown of α-SMA alone confers clonogenicity and adipogenic/osteogenic differentiation suggest that the MF is an activated phenotype and not a terminal differentiation state of SMA(+) hMSCs.

Expression of α-SMA in hMSCs Controls YAP/TAZ Nuclear Localization

We next addressed how α-SMA regulates hMSC fate and clonogenicity. Cell contractility and actin filament bundle assembly both stimulate activation and translocation of YAP/TAZ to the nucleus (Dupont et al., 2011; Gaspar and Tapon, 2014). YAP/TAZ transcriptionally regulate genes associated with stem cell fate decision and self-renewal (Varelas, 2014). To test whether α-SMA expression affects YAP/TAZ localization in hMSCs, we first co-analyzed α-SMA stress fiber intensity with the ratio of nuclear/cytosolic YAP on an individual cell basis and demonstrated a clear correlation (Figure S5). The low baseline percentage of SMA(−) hMSCs with predominantly nuclear YAP (25%, nuclear/cytosolic YAP > 1) was increased to 90% after transfection with α-SMA-GFP, corresponding to the percentage of SMA(+) hMSCs with constitutive nuclear YAP (Figure 5A). Knockdown of α-SMA with shRNA reduced the percentage of SMA(+) hMSCs with predominantly nuclear YAP to 7% (Figure 5B).

To decipher the mode of action of α-SMA, contraction, or action polymerization, we used the α-SMA-specific fusion peptide SMA-FP in combination with cytoskeletal drugs (Figure 5C). SMA-FP selectively targets α-SMA in stress fibers, inhibits α-SMA-mediated contraction, and selectively depolymerizes α-SMA from stress fibers (Clément et al., 2005; Hinz et al., 2002). SMA-FP removed α-SMA from persisting stress fibers, in contrast to control (DMSO and skeletal actin fusion peptide, SKA-FP) SMA(+) hMSCs (Figure S5). SMA-FP treatment resulted in low levels of nuclear YAP and reduced hMSC contraction on wrinkling elastomer substrates (Figure 5C). SMA(+) hMSCs treated with the myosin II inhibitor blebbistatin showed similar low levels of YAP in the nucleus and low contraction, but disassembled all actins from stress fibers, as evident from phalloidin staining (Figures 5C and S5).

Next, we stabilized stress fibers by pre-treating SMA(+) hMSCs with jasplakinolide, followed by addition of SMA-FP (Figure 5D). With jasplakinolide being present, the SMA-FP was unable to depolymerize α-SMA from stress fibers (Figure 5D) and hMSCs contraction was unaltered (Figures 5D and 5E), indicating that the SMA-FP reduces MF contraction primarily by depolymerizing α-SMA from stress fibers. Whereas YAP nuclear localization remained high under jasplakinolide/SMA-FP treatment (Figures 5D and 5F), addition of blebbistatin to jasplakinolide-treated SMA(+) hMSCs resulted in the loss of α-SMA from stress fibers, reduced cell contractility, and reduced YAP nuclear localization (Figures 5D–5F). Control SMA(+) hMSCs treated with jasplakinolide alone were similar to untreated cells (Figures 5D–5F). In combination, these experiments suggest that enhanced contractile activity mediated by α-SMA upregulates YAP/TAZ nuclear localization.

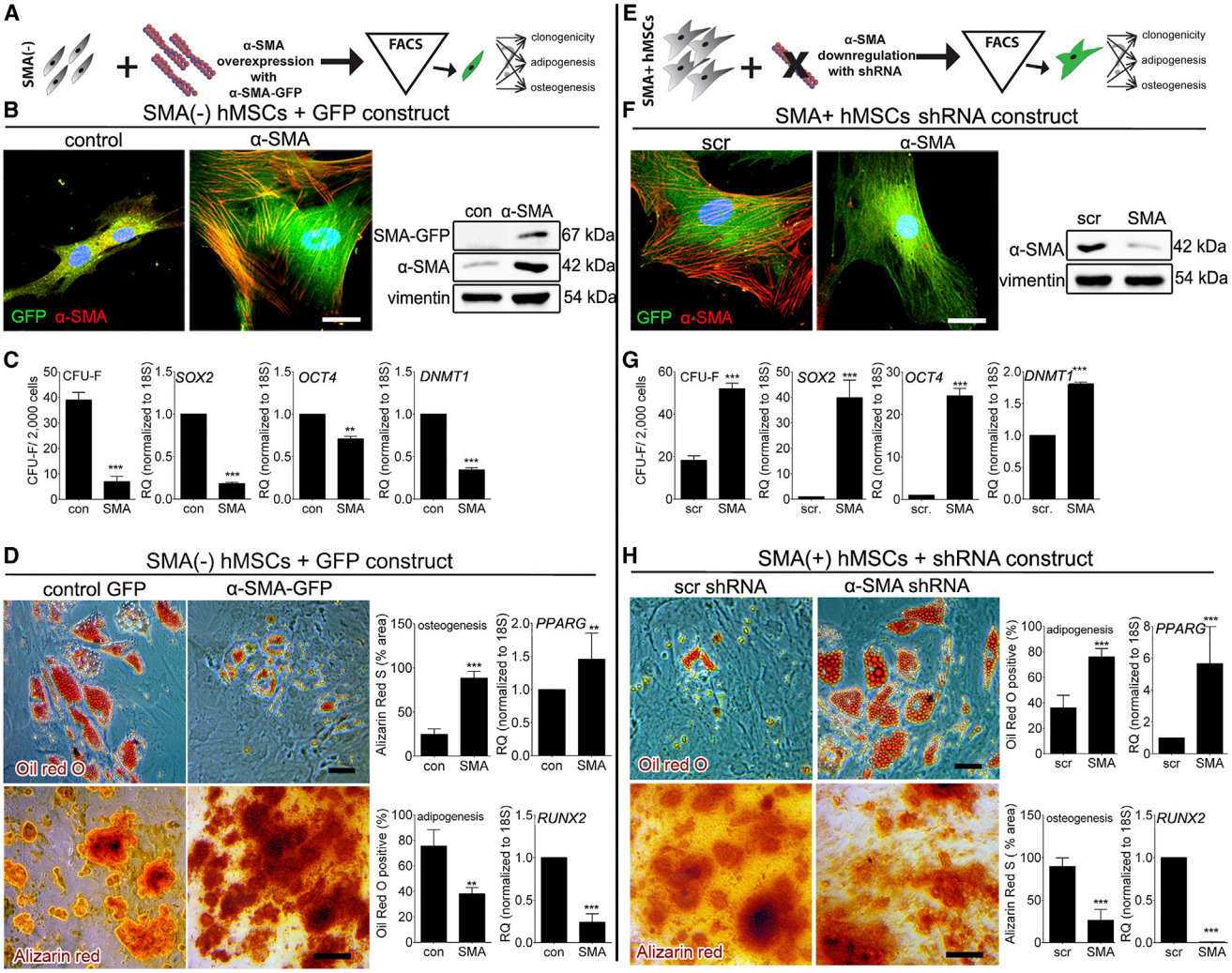

Figure 4. Overexpression and Knockdown of α-SMA Affecs hMSC Stem Cell Character

(A) SMA(−) hMSCs were transfected with control GFP or α-SMA-GFP constructs and evaluated for clonogenicity and lineage differentiation.

(B) Transfected cells were cultured for 5 days and stained for α-SMA (red) and GFP (green) (the scale bar represents 20 μm) and processed for western blotting.

(C) The effect of α-SMA overexpression on stem cell character was assessed by CFU-F assays and qRT-PCR analysis of *SOX2*, *OCT4*, and *DNMT1*.

(D) Differentiation potential was tested by inducing adipogenic and osteogenic lineages using respective induction media and assessed for adipogenesis and osteogenesis. The scale bar represents 50 μm.

(E–H) The same analysis was performed with SMA(+) hMSCs that were transfected with either scrambled (scr) shRNA or α-SMA-shRNA constructs.

The graphs show averages ± SD from at least three independent experiments (*$p \leq 0.05$, **$p \leq 0.005$, and ***$p \leq 0.0005$ using Student's t test). See also Figure S4.

To show that YAP/TAZ activation is indeed responsible for reduced lineage differentiation and self-renewal capacity downstream of α-SMA-expression in hMSCs, we co-transfected SMA(−) hMSCs with small interfering (si) RNA directed against YAP1 together with α-SMA-GFP. Transfection of YAP1 siRNA substantially reduced YAP expression levels (Figure 6A) and resulted in reduced *RUNX2* mRNA levels, increased *PPARG* mRNA, and reduced *SOX2* and *OCT4* levels in control cells (Figure 6A, GFP). Knockdown of YAP1 in α-SMA-overexpressing hMSCs restored expression of *PPARG* mRNA and strongly reduced *RUNX2* mRNA expression (Figure 6A). These results confirmed that the effect of high α-SMA expression on hMSC lineage differentiation potential is mediated by YAP. However, knockdown of YAP1 in α-SMA-overexpressing hMSCs did not restore high expression of *SOX2* and

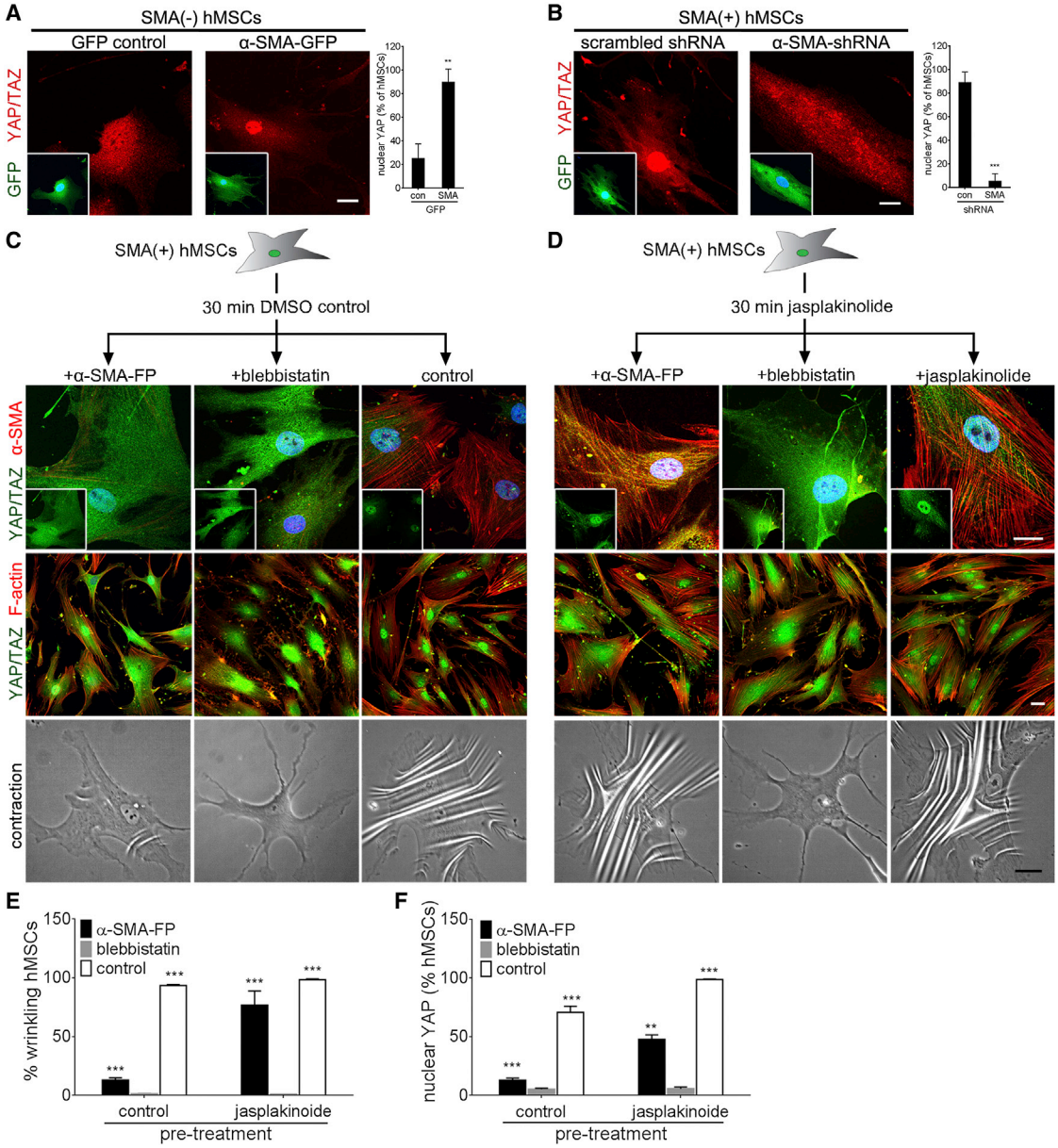

Figure 5. Presence of α-SMA in hMSC Stress Fibers Results in YAP/TAZ Nuclear Accumulation

(A) Sorted SMA(−) hMSCs were transfected with control GFP and α-SMA-GFP constructs.

(B) Sorted SMA(+) hMSCs were transfected with control scrambled (scr) and α-SMA-shRNA constructs. Localization of YAP/TAZ was visualized using immunofluorescence staining for YAP (red) and GFP (green).

(C–F) The ratio of nuclear over cytosolic YAP/TAZ was calculated by image analysis and the percentage of cells with predominantly nuclear YAP/TAZ localization was determined. Sorted SMA(+) cells were either pre-treated with (C) DMSO (control) or (D) jasplakinolide for 30 min, followed by the addition of the α-SMA N-terminal peptide AcEEED (SMA-FP), blebbistatin, or DMSO control for another 40 min. Cells were then stained for YAP and α-SMA or YAP and stress fibers as indicated and assessed for contraction using wrinkling silicone substrates. Quantified from these images were (E) cell contraction as percentage of cells associated with wrinkles, and (F) percentage of cells with predominant nuclear YAP/TAZ localization.

All scale bars represent 20 μm. The graphs show averages ± SD from at least three independent experiments (*$p \leq 0.05$ and **$p \leq 0.005$ using ANOVA followed by a post hoc Tukey's multiple comparison test). See also Figure S5.

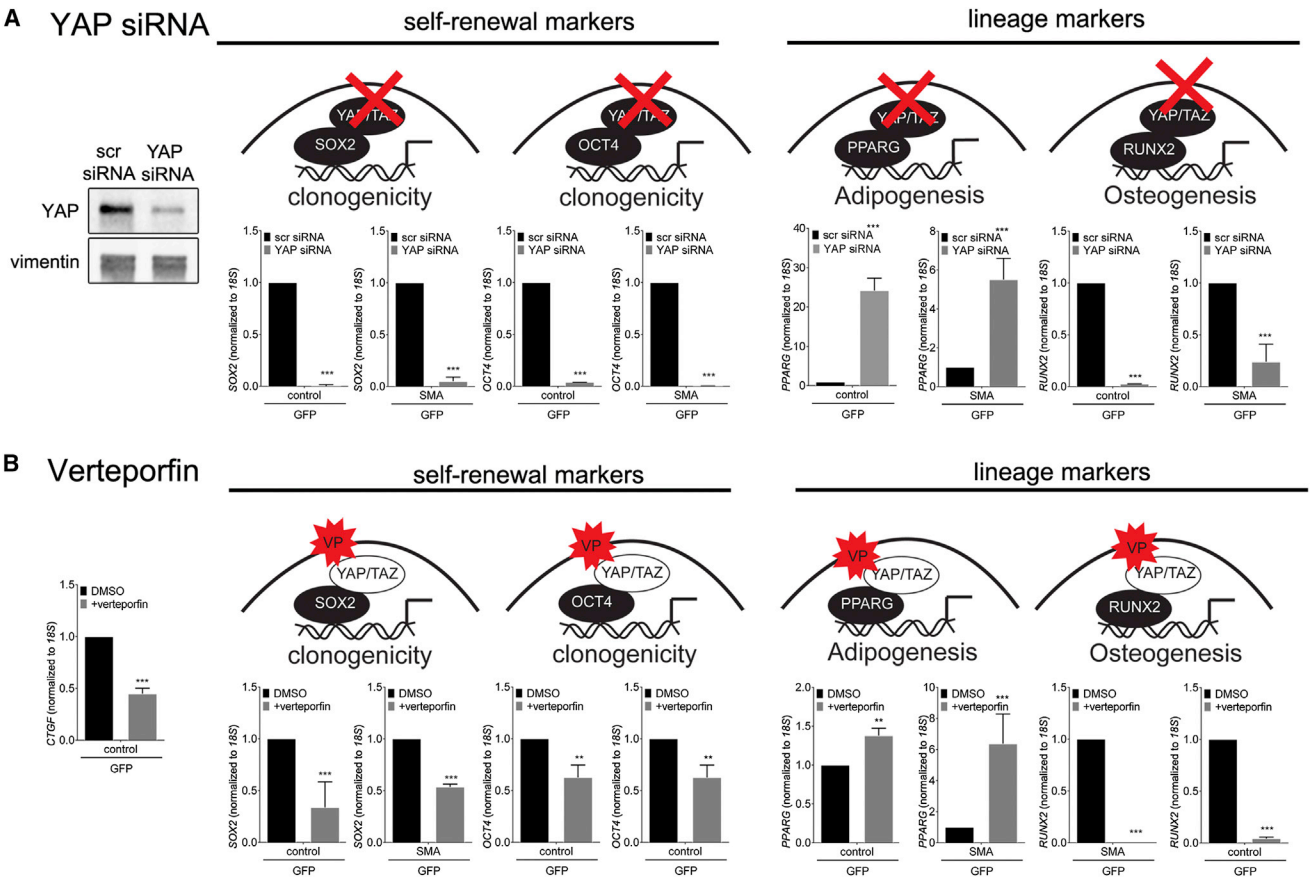

Figure 6. Suppression of MSC Adipogenesis by α-SMA Is Mediated via YAP

(A) Sorted SMA(−) hMSCs were co-transfected with siRNA directed against YAP1 together with control GFP or α-SMA-GFP constructs and assessed after 5 days. YAP downregulation was confirmed using western blotting.

(B) Sorted SMA(−) hMSCs were transfected with control GFP or α-SMA-GFP constructs and treated for 5 days with verteporfin (VP, 2 μM) or DMSO control. Efficacy of vereporfin was assessed by performing qRT-PCR for the YAP1 downstream target CCN2 (CTGF). All cells were analyzed by qRT-PCR for mRNA expression of *RUNX2*, *PPARG*, *SOX2*, and *OCT4*.

The graphs show averages ± SD from three different donors per condition (*p ≤ 0.05, **p ≤ 0.005, and ***p ≤ 0.0005 using ANOVA followed by a post hoc Tukey's multiple comparison test).

OCT4, as expected if α-SMA would suppress hMSC self-renewal by acting through YAP1 (Figure 6A). To test whether this result was due to the overall loss of YAP, we used verteporfin to selectively abrogate the nuclear activity of YAP by inhibiting binding to TEAD elements (Liu-Chittenden et al., 2012) (Figure 6B). Drug action was controlled by low levels of the YAP1 downstream target CCN2 (CTGF) (Figure 6B). Treating SMA(−) and SMA(−)-overexpressing α-SMA with verteporfin generally confirmed our results obtained with YAP1 knockdown (Figure 6B). Hence, α-SMA expression levels regulate the hMSC multilineage differentiation program via YAP, but downregulate hMSC self-renewal possibly through a different mechanism.

Finally, to investigate whether α-SMA expression is relevant for YAP/TAZ activation and hMSC lineage determination in vivo, we correlated α-SMA expression and YAP nuclear localization in soft mesenchymal tumors (adiposarcoma) and stiff mesenchymal tumors (osteosarcoma) that involve MSC tumorigenesis and fibrogenesis (Mohseny et al., 2009; Rodriguez et al., 2012; Xiao et al., 2013). The levels of α-SMA expression were negligible in healthy fat control tissue and low in normal bone, but significantly higher in the activated stroma of the respective tumor (Figures 7A–7C). Increased α-SMA expression in adiposarcoma correlated with 3.5-fold higher percentages of cells with predominantly nuclear YAP staining (22%) compared to normal fat tissue (6%, Figures 7A, 7C, and 7D). The levels of nuclear localized YAP staining did not significantly increase in osteosarcoma compared to already high levels observed in healthy bone (Figures 7B–7D), supporting that high levels of YAP/TAZ in mesenchymal cells direct osteogenic differentiation.

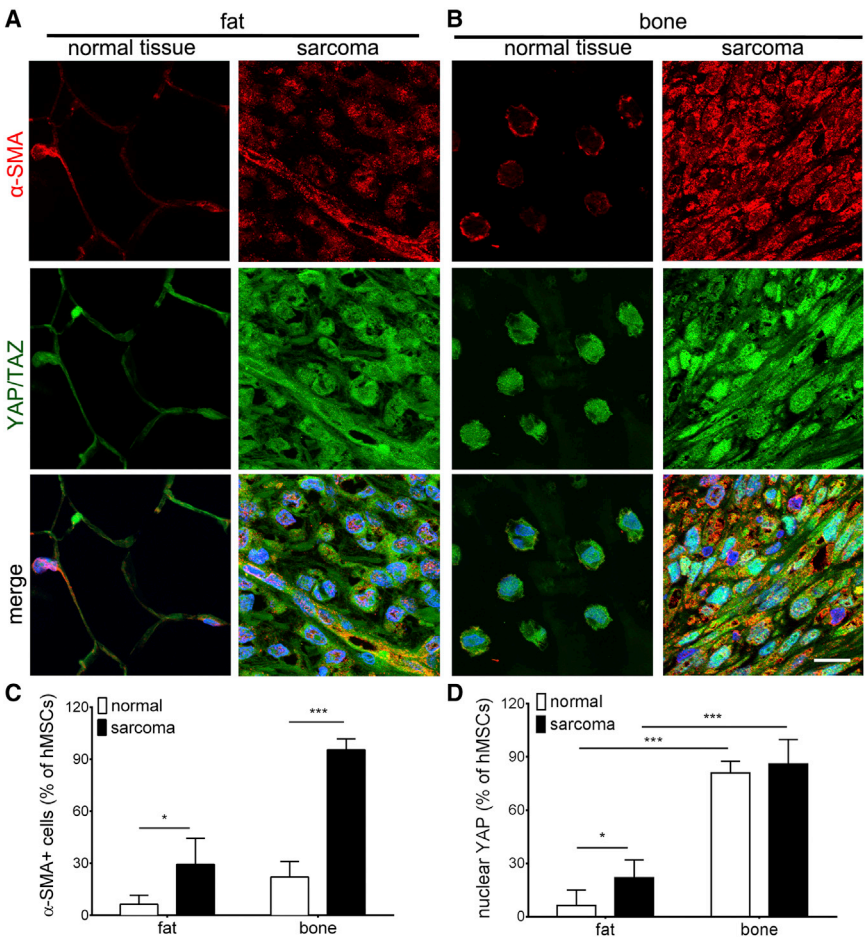

Figure 7. Expression of α-SMA Correlates with High Levels of Nuclear YAP/TAZ in Human Adiposarcoma and Osteosarcoma Tissues

(A) Human normal fat and adiposarcoma tissue samples were obtained from the same donor, sectioned, and stained for α-SMA (red), YAP (green), and cell nuclei (blue).

(B) Donor-matched normal bone and osteosarcoma tissue were similarly processed.

(C and D) Percentage of (C) α-SMA-positive cells and (D) cells with predominantly nuclear YAP were quantified from at least three tissue sections per donor. The graphs show averages ± SD from three different donors per condition (*$p \leq 0.05$, **$p \leq 0.005$, and ***$p \leq 0.0005$ using ANOVA followed by a post hoc Tukey's multiple comparison test).

DISCUSSION

MSCs are prone to MF activation by stiff ECM and TGF-β1, but the consequences on their stem cell potential and reversibility have not been systematically assessed. We establish a direct link between α-SMA expression/function, YAP/TAZ activity, and hMSC fate. Different actin isoforms promote specific types of actin organization levels and a shift in the ratios of actin isoforms can reprogram cell differentiation (Lechuga et al., 2014; Tondeleir et al., 2012). α-SMA incorporation into existing stress fibers has been shown to increase actin organization and intracellular tension (Goffin et al., 2006; Hinz et al., 2001). Actin organization as cortical filaments or incorporation into stress fiber bundles has been shown to differentially control YAP/TAZ activation, nuclear localization, and regulation of the Hippo pathway (Gaspar and Tapon, 2014; Halder et al., 2012; Yu et al., 2012a). In epithelia, cell-morphology-dependent actin organization provides positional information to individual cells in a multicellular layer (Aragona et al., 2013; Wada et al., 2011). YAP/TAZ are also central in regulating cell fate decision by interacting with *RUNX2* and *PPARG* (Hong et al., 2005; Hong and Yaffe, 2006; Varelas et al., 2008). Consistently, neo-expression of α-SMA alone was sufficient in our experiments to reduce hMSC differentiation potential, which was rescued by inhibition and downregulation of YAP1.

Whether the α-SMA-induced nuclear shift of YAP is responsible for reduced clonogenicity is unclear because YAP1 knockdown did not protect against the reduction of *SOX2* and *OCT4* transcript levels upon α-SMA-overexpression. Consistently, YAP binds to and is expected to activate gene transcription of *SOX2* and *OCT4* in embryonic stem (ES) cells (Lian et al., 2010). However, YAP is inactivated in ES cells during differentiation (Lian et al., 2010), whereas it drives specific lineage specification in MSCs (Dupont et al., 2011). Overexpression of *OCT4* has been shown to result in increased MSC proliferation, whereas *OCT4* knockdown had the opposite effect (Tsai et al., 2012). Similarly, knockdown of *SOX2* reduces proliferation in MSC-derived osteoprogenitors that is restored by YAP1 overexpression, which acts downstream of *SOX2* in this

model (Seo et al., 2013). Hence, the interplay between α-SMA, YAP/TAZ, and self-renewal genes is complex and not entirely understood at present.

YAP/TAZ transcription factors provide a direct link between cell mechanosensing and gene regulation (Halder et al., 2012). Inhibition of cell contraction has been shown to decrease nuclear localization of YAP/TAZ and transcription of downstream genes, whereas high intracellular tension drives YAP/TAZ into the nucleus (Calvo et al., 2013; Dupont et al., 2011). Expression of α-SMA is not essential for the localization of YAP/TAZ in the nucleus and ~10% of the hMSC retained predominantly nuclear YAP even in the presence of the SMA-FP. However, incorporation of α-SMA into existing stress fibers substantially increases contractile force and cell stress (Hinz et al., 2001) and thus accentuates fibrogenic transcription programs. YAP/TAZ have been shown to be involved in regulating α-SMA expression and fibrogenesis using an experimental model of epithelial-to-mesenchymal transition (Speight et al., 2013) and during lung fibroblast-to-MF activation by stiff ECM (Liu et al., 2015). These reports and our works suggest a positive feedback loop between α-SMA and YAP/TAZ signaling that amplifies fibrosis.

Importantly, expression of α-SMA is not simply a marker for MF activation, but also the driver of cell function and fate. Increased expression of α-SMA directly reduces the clonal potential of hMSCs and guides their differentiation toward osteoblasts. Hence, α-SMA not only identifies osteoprogenitors in hMSC populations as shown by others before (Grcevic et al., 2012; Kalajzic et al., 2008), but may be part of the mechanism driving differentiation. Analysis of bone marrow-derived hMSCs treated with TGF-β1 and/or exposed to fibrosis-stiff culture substrates has previously revealed a fibrogenic MF activation program (Park et al., 2011; Wang et al., 2004). Our results additionally demonstrate that neo-expression of α-SMA associates with reduced clonogenicity and lineage differentiation potential of hMSCs and that this program is reversible. SMA(+) hMSC can be deactivated to lose fibrotic MF features by reducing substrate stiffness. Originally considered to be a terminal differentiation state of various precursor cells, deactivation of the MF has been shown in recent experimental models of kidney and liver fibrosis (Hecker et al., 2011; Kisseleva and Brenner, 2013). In vitro, the depletion of MF features in fibroblasts and MSCs is achieved by culture on soft silicone substrates (Achterberg et al., 2014; Balestrini et al., 2012; Goffin et al., 2006; Park et al., 2011) or by treatment with anti-fibrotic growth factors (Desai et al., 2014). Our results add to these findings that SMA(+) hMSC populations, deactivated to lose MF features, regain adipogenic lineage differentiation potential rather than turning into α-SMA-negative fibroblasts. Hence, α-SMA-positive cells are likely derived from previously α-SMA-negative hMSCs and expression of α-SMA reversibly reduced their clonogenicity and lineage potential.

Our findings have important implications for hMSC therapy in fibroproliferative diseases, including tumor formation and development of fibrosis. Our in vivo data show that the percentage of α-SMA-expressing MFs in sarcomas correlates with the degree of YAP/TAZ activation. A wide variety of different tumors have been shown to accumulate stromal cells that are positive for α-SMA and perform MF functions, including stiffening of the stroma and promoting tumor progression (Hinz et al., 2012; Öhlund et al., 2014). Consistently, YAP expressed in cancer-associated fibroblasts was recently shown to play an important role in controlling of cytoskeleton-regulating genes, as well as tumor cell invasion and ECM stiffening (Calvo et al., 2013). We propose a feedforward loop of MSC-to-MF activation in the tumor microenvironment, leading to higher contractile cells and stiffer ECM, which both lead to increased YAP/TAZ activity and conversion of regenerative MSCs into fibrotic MFs.

Interrupting this feedforward loop will have important consequences for hMSC potential in clinical applications. First, specific inhibitors of α-SMA such as the SMA-FP or shRNA strategies may be co-delivered with hMSCs to exert fibrosis-inhibitory effects on the resident fibrotic cell population in the lesion. Second, suppressing MSC-to-MF activation during cell culture expansion will enhance the fraction of valuable stem cells and reduce the risk of fibrosis upon implantation. We have shown that explantation and continued culture on soft culture substrates renders populations of lung fibroblasts resistant to subsequent mechanical activation on stiff substrates over several consecutive passages (Balestrini et al., 2012). This concept of cells acquiring a "mechanical memory" has recently been confirmed for MSC lineage programs on a shorter timescale with YAP/TAZ being involved (Yang et al., 2014). It is yet unclear why hMSCs and other mesenchymal cells that have been cultured on conventional stiff culture dishes are not similarly primed and can at least acutely (up to 8 days in our experiments) lose fibrogenic character upon short-term exposure (5 days) to soft substrates. In our own studies, we found it to be essential to use substrates with a pathophysiological stiffness range (1–100 kPa) and to never expose cells to tissue culture plastic for mechanical priming to occur (Balestrini et al., 2012).

EXPERIMENTAL PROCEDURES

For detailed experimental procedures, see the Supplemental Experimental Procedures.

Tissue, Cell Culture, and Drugs

MSCs were obtained from the bone marrow of healthy donors (Davies et al., 2001), from umbilical perivasculature (Ennis et al., 2008)

and from adipose tissue (Vermette et al., 2007). Tissue sections of mesenchymal tumors and respective healthy control tissues were purchased from Biomax. Cell drugs used in these study are: blebbistatin (50 μM) (Tocris Bioscience, Cedarlane), jasplakinolide (50 nM) (Life Technologies), verteporfin (2 μM) (Sigma-Aldrich), SMA-FP and control SKA-FP (5 μM). Immunofluorescence, microscopy, and western blot were performed as described earlier with antibodies listed in the Supplemental Experimental Procedures (Klingberg et al., 2014). Adipogenesis, osteogenesis, and chondrogenesis were induced and assessed as described earlier (Majd et al., 2011). Elastic silicone culture substrates were purchased from Excellness Biotech SA and activated for cell adhesion by plasma oxygenation (PE-100, Plasma Etch), followed by coating with 2 μg/cm^2 FN (Millipore). Cell contractility was assessed using FN-coated wrinkling silicone substrates (Balestrini et al., 2012).

Flow Cytometry and Cell Sorting

For flow cytometry, fixed cells were immunostained using antibodies CD44-APC-H7, CD73-PE-CY7, CD90-FITC, CD105-PerCP-Cy5.5, CD146-V450, and respective isotype controls (BD Bioscience) and analyzed using a flow cytometer (LSR II, BD). To enrich for α-SMA-positive and α-SMA-negative hMSC populations, cells were trypsinized and sorted for cell size (upper and lower 25% in forward scatter) using fluorescence activated cell sorting (FACS) (FACSAria III, BD).

Plasmid Constructs

α-SMA was overexpressed using α-SMA-GFP (Clément et al., 2005) and knockeddown using 29-mer shRNA targeting α-SMA transcripts in pGFP-V-RS vectors (OriGene Technologies). Human YAP1 27-mer siRNA were ordered from (OriGene Technologies). Cells were transfected using an electroporation device (Neon, Life Technologies).

SUPPLEMENTAL INFORMATION

Supplemental Information includes Supplemental Experimental Procedures and five figures and can be found with this article online at http://dx.doi.org/10.1016/j.stemcr.2015.05.004.

AUTHOR CONTRIBUTIONS

N.P.T. designed, performed, analyzed, and wrote the experimental data in manuscript format. B.H. supervised, designed, analyzed, and wrote the manuscript. J.F., J.E.D., and A.K. contributed to data analysis and writing of the manuscript.

ACKNOWLEDGMENTS

We thank Drs. Christine Chaponnier and Giulio Gabbiani for kindly providing anti-α-SMA antibody and SMA/SKA fusion peptides. We are also thankful to Stellar Boo for technical support. We are grateful to Dr. Chris McCulloch (University of Toronto, Toronto) for carefully reading our manuscript and his invaluable input. This research was supported by the Canadian Institutes of Health Research (CIHR) (grants #210820 and #286920 to B.H. and #111233 to J.F.), the Collaborative Health Research Programme (CIHR/NSERC) (#1004005 and #413783), and the Canada Foundation for Innovation and Ontario Research Fund (CFI/ORF) (#26653) all to B.H. N.P.T. was a Marie Curie Fellow at the Tissue Transmigration Training Network (T3-Net) funded by the European Commission under Framework Program (FP7/2007-2013) with grant agreement #237946 and the University of Toronto Fellowship.

Received: November 19, 2014
Revised: May 4, 2015
Accepted: May 4, 2015
Published: May 28, 2015

REFERENCES

Achterberg, V.F., Buscemi, L., Diekmann, H., Smith-Clerc, J., Schwengler, H., Meister, J.J., Wenck, H., Gallinat, S., and Hinz, B. (2014). The nano-scale mechanical properties of the extracellular matrix regulate dermal fibroblast function. J. Invest. Dermatol. *134*, 1862–1872.

Aragona, M., Panciera, T., Manfrin, A., Giulitti, S., Michielin, F., Elvassore, N., Dupont, S., and Piccolo, S. (2013). A mechanical checkpoint controls multicellular growth through YAP/TAZ regulation by actin-processing factors. Cell *154*, 1047–1059.

Arnold, K., Sarkar, A., Yram, M.A., Polo, J.M., Bronson, R., Sengupta, S., Seandel, M., Geijsen, N., and Hochedlinger, K. (2011). Sox2(+) adult stem and progenitor cells are important for tissue regeneration and survival of mice. Cell Stem Cell *9*, 317–329.

Balestrini, J.L., Chaudhry, S., Sarrazy, V., Koehler, A., and Hinz, B. (2012). The mechanical memory of lung myofibroblasts. Integr. Biol. (Camb) *4*, 410–421.

Behfar, A., Crespo-Diaz, R., Terzic, A., and Gersh, B.J. (2014). Cell therapy for cardiac repair—lessons from clinical trials. Nat. Rev. Cardiol. *11*, 232–246.

Bianco, P., Cao, X., Frenette, P.S., Mao, J.J., Robey, P.G., Simmons, P.J., and Wang, C.Y. (2013). The meaning, the sense and the significance: translating the science of mesenchymal stem cells into medicine. Nat. Med. *19*, 35–42.

Breitbach, M., Bostani, T., Roell, W., Xia, Y., Dewald, O., Nygren, J.M., Fries, J.W., Tiemann, K., Bohlen, H., Hescheler, J., et al. (2007). Potential risks of bone marrow cell transplantation into infarcted hearts. Blood *110*, 1362–1369.

Calvo, F., Ege, N., Grande-Garcia, A., Hooper, S., Jenkins, R.P., Chaudhry, S.I., Harrington, K., Williamson, P., Moeendarbary, E., Charras, G., and Sahai, E. (2013). Mechanotransduction and YAP-dependent matrix remodelling is required for the generation and maintenance of cancer-associated fibroblasts. Nat. Cell Biol. *15*, 637–646.

Clément, S., Hinz, B., Dugina, V., Gabbiani, G., and Chaponnier, C. (2005). The N-terminal Ac-EEED sequence plays a role in alpha-smooth-muscle actin incorporation into stress fibers. J. Cell Sci. *118*, 1395–1404.

Davies, J.E., Baksh, D., and Karp, J.M. (2001). Mesenchymal cell culture: bone. In Methods in Tissue Engineering, A. Atala and R. Lanza, eds. (San Diego: Academic Press), pp. 333–344.

Desai, V.D., Hsia, H.C., and Schwarzbauer, J.E. (2014). Reversible modulation of myofibroblast differentiation in adipose-derived mesenchymal stem cells. PLoS ONE *9*, e86865.

di Bonzo, L.V., Ferrero, I., Cravanzola, C., Mareschi, K., Rustichell, D., Novo, E., Sanavio, F., Cannito, S., Zamara, E., Bertero, M., et al. (2008). Human mesenchymal stem cells as a two-edged sword in hepatic regenerative medicine: engraftment and hepatocyte differentiation versus profibrogenic potential. Gut *57*, 223–231.

Dupont, S., Morsut, L., Aragona, M., Enzo, E., Giulitti, S., Cordenonsi, M., Zanconato, F., Le Digabel, J., Forcato, M., Bicciato, S., et al. (2011). Role of YAP/TAZ in mechanotransduction. Nature *474*, 179–183.

Engler, A.J., Sen, S., Sweeney, H.L., and Discher, D.E. (2006). Matrix elasticity directs stem cell lineage specification. Cell *126*, 677–689.

Ennis, J., Sarugaser, R., Gomez, A., Baksh, D., and Davies, J.E. (2008). Isolation, characterization, and differentiation of human umbilical cord perivascular cells (HUCPVCs). Methods Cell Biol. *86*, 121–136.

Fernández, P., Perez-Aso, M., Smith, G., Wilder, T., Trzaska, S., Chiriboga, L., Franks, A., Jr., Robson, S.C., Cronstein, B.N., and Chan, E.S. (2013). Extracellular generation of adenosine by the ectonucleotidases CD39 and CD73 promotes dermal fibrosis. Am. J. Pathol. *183*, 1740–1746.

Forbes, S.J., and Rosenthal, N. (2014). Preparing the ground for tissue regeneration: from mechanism to therapy. Nat. Med. *20*, 857–869.

Gaspar, P., and Tapon, N. (2014). Sensing the local environment: actin architecture and Hippo signalling. Curr. Opin. Cell Biol. *31*, 74–83.

Goffin, J.M., Pittet, P., Csucs, G., Lussi, J.W., Meister, J.J., and Hinz, B. (2006). Focal adhesion size controls tension-dependent recruitment of alpha-smooth muscle actin to stress fibers. J. Cell Biol. *172*, 259–268.

Grcevic, D., Pejda, S., Matthews, B.G., Repic, D., Wang, L., Li, H., Kronenberg, M.S., Jiang, X., Maye, P., Adams, D.J., et al. (2012). In vivo fate mapping identifies mesenchymal progenitor cells. Stem Cells *30*, 187–196.

Halder, G., Dupont, S., and Piccolo, S. (2012). Transduction of mechanical and cytoskeletal cues by YAP and TAZ. Nat. Rev. Mol. Cell Biol. *13*, 591–600.

Hecker, L., Jagirdar, R., Jin, T., and Thannickal, V.J. (2011). Reversible differentiation of myofibroblasts by MyoD. Exp. Cell Res. *317*, 1914–1921.

Hinz, B. (2010a). The myofibroblast in connective tissue repair and regeneration. In Regenerative Medicine and Biomaterials for the Repair of Connective Tissues, C.A.J. Ralphs, ed. (Cambridge: Woodhead Publishing), pp. 39–82.

Hinz, B. (2010b). The myofibroblast: paradigm for a mechanically active cell. J. Biomech. *43*, 146–155.

Hinz, B., Celetta, G., Tomasek, J.J., Gabbiani, G., and Chaponnier, C. (2001). Alpha-smooth muscle actin expression upregulates fibroblast contractile activity. Mol. Biol. Cell *12*, 2730–2741.

Hinz, B., Gabbiani, G., and Chaponnier, C. (2002). The NH2-terminal peptide of alpha-smooth muscle actin inhibits force generation by the myofibroblast in vitro and in vivo. J. Cell Biol. *157*, 657–663.

Hinz, B., Phan, S.H., Thannickal, V.J., Prunotto, M., Desmoulière, A., Varga, J., De Wever, O., Mareel, M., and Gabbiani, G. (2012). Recent developments in myofibroblast biology: paradigms for connective tissue remodeling. Am. J. Pathol. *180*, 1340–1355.

Hong, J.H., and Yaffe, M.B. (2006). TAZ: a beta-catenin-like molecule that regulates mesenchymal stem cell differentiation. Cell Cycle *5*, 176–179.

Hong, J.H., Hwang, E.S., McManus, M.T., Amsterdam, A., Tian, Y., Kalmukova, R., Mueller, E., Benjamin, T., Spiegelman, B.M., Sharp, P.A., et al. (2005). TAZ, a transcriptional modulator of mesenchymal stem cell differentiation. Science *309*, 1074–1078.

Kalajzic, Z., Li, H., Wang, L.P., Jiang, X., Lamothe, K., Adams, D.J., Aguila, H.L., Rowe, D.W., and Kalajzic, I. (2008). Use of an alpha-smooth muscle actin GFP reporter to identify an osteoprogenitor population. Bone *43*, 501–510.

Karnoub, A.E., Dash, A.B., Vo, A.P., Sullivan, A., Brooks, M.W., Bell, G.W., Richardson, A.L., Polyak, K., Tubo, R., and Weinberg, R.A. (2007). Mesenchymal stem cells within tumour stroma promote breast cancer metastasis. Nature *449*, 557–563.

Kim, W., Barron, D.A., San Martin, R., Chan, K.S., Tran, L.L., Yang, F., Ressler, S.J., and Rowley, D.R. (2014). RUNX1 is essential for mesenchymal stem cell proliferation and myofibroblast differentiation. Proc. Natl. Acad. Sci. USA *111*, 16389–16394.

Kisseleva, T., and Brenner, D.A. (2013). Inactivation of myofibroblasts during regression of liver fibrosis. Cell Cycle *12*, 381–382.

Klingberg, F., Chow, M.L., Koehler, A., Boo, S., Buscemi, L., Quinn, T.M., Costell, M., Alman, B.A., Genot, E., and Hinz, B. (2014). Prestress in the extracellular matrix sensitizes latent TGF-β1 for activation. J. Cell Biol. *207*, 283–297.

Koumas, L., Smith, T.J., Feldon, S., Blumberg, N., and Phipps, R.P. (2003). Thy-1 expression in human fibroblast subsets defines myofibroblastic or lipofibroblastic phenotypes. Am. J. Pathol. *163*, 1291–1300.

Lechuga, S., Baranwal, S., Li, C., Naydenov, N.G., Kuemmerle, J.F., Dugina, V., Chaponnier, C., and Ivanov, A.I. (2014). Loss of γ-cytoplasmic actin triggers myofibroblast transition of human epithelial cells. Mol. Biol. Cell *25*, 3133–3146.

Li, Y., Jiang, D., Liang, J., Meltzer, E.B., Gray, A., Miura, R., Wogensen, L., Yamaguchi, Y., and Noble, P.W. (2011). Severe lung fibrosis requires an invasive fibroblast phenotype regulated by hyaluronan and CD44. J. Exp. Med. *208*, 1459–1471.

Lian, I., Kim, J., Okazawa, H., Zhao, J., Zhao, B., Yu, J., Chinnaiyan, A., Israel, M.A., Goldstein, L.S., Abujarour, R., et al. (2010). The role of YAP transcription coactivator in regulating stem cell self-renewal and differentiation. Genes Dev. *24*, 1106–1118.

Liu, F., Lagares, D., Choi, K.M., Stopfer, L., Marinkovic, A., Vrbanac, V., Probst, C.K., Hiemer, S.E., Sisson, T.H., Horowitz, J.C., et al. (2015). Mechanosignaling through YAP and TAZ drives fibroblast activation and fibrosis. Am. J. Physiol. Lung Cell. Mol. Physiol. *308*, L344–L357.

Liu-Chittenden, Y., Huang, B., Shim, J.S., Chen, Q., Lee, S.J., Anders, R.A., Liu, J.O., and Pan, D. (2012). Genetic and pharmacological disruption of the TEAD-YAP complex suppresses the oncogenic activity of YAP. Genes Dev. *26*, 1300–1305.

MacQueen, L., Sun, Y., and Simmons, C.A. (2013). Mesenchymal stem cell mechanobiology and emerging experimental platforms. J. R. Soc. Interface *10*, 20130179.

Majd, H., Quinn, T.M., Wipff, P.J., and Hinz, B. (2011). Dynamic expansion culture for mesenchymal stem cells. Methods Mol. Biol. *698*, 175–188.

Maring, J.A., Trojanowska, M., and ten Dijke, P. (2012). Role of endoglin in fibrosis and scleroderma. Int. Rev. Cell Mol. Biol. *297*, 295–308.

McBeath, R., Pirone, D.M., Nelson, C.M., Bhadriraju, K., and Chen, C.S. (2004). Cell shape, cytoskeletal tension, and RhoA regulate stem cell lineage commitment. Dev. Cell *6*, 483–495.

McQualter, J.L., McCarty, R.C., Van der Velden, J., O'Donoghue, R.J., Asselin-Labat, M.L., Bozinovski, S., and Bertoncello, I. (2013). TGF-β signaling in stromal cells acts upstream of FGF-10 to regulate epithelial stem cell growth in the adult lung. Stem Cell Res. (Amst.) *11*, 1222–1233.

Mishra, P.J., Mishra, P.J., Glod, J.W., and Banerjee, D. (2009). Mesenchymal stem cells: flip side of the coin. Cancer Res. *69*, 1255–1258.

Mohseny, A.B., Szuhai, K., Romeo, S., Buddingh, E.P., Briaire-de Bruijn, I., de Jong, D., van Pel, M., Cleton-Jansen, A.M., and Hogendoorn, P.C. (2009). Osteosarcoma originates from mesenchymal stem cells in consequence of aneuploidization and genomic loss of Cdkn2. J. Pathol. *219*, 294–305.

Nagaya, N., Kangawa, K., Itoh, T., Iwase, T., Murakami, S., Miyahara, Y., Fujii, T., Uematsu, M., Ohgushi, H., Yamagishi, M., et al. (2005). Transplantation of mesenchymal stem cells improves cardiac function in a rat model of dilated cardiomyopathy. Circulation *112*, 1128–1135.

Ninichuk, V., Gross, O., Segerer, S., Hoffmann, R., Radomska, E., Buchstaller, A., Huss, R., Akis, N., Schlöndorff, D., and Anders, H.J. (2006). Multipotent mesenchymal stem cells reduce interstitial fibrosis but do not delay progression of chronic kidney disease in collagen4A3-deficient mice. Kidney Int. *70*, 121–129.

Öhlund, D., Elyada, E., and Tuveson, D. (2014). Fibroblast heterogeneity in the cancer wound. J. Exp. Med. *211*, 1503–1523.

Park, J.S., Chu, J.S., Tsou, A.D., Diop, R., Tang, Z., Wang, A., and Li, S. (2011). The effect of matrix stiffness on the differentiation of mesenchymal stem cells in response to TGF-β. Biomaterials *32*, 3921–3930.

Prockop, D.J., Prockop, S.E., and Bertoncello, I. (2014). Are clinical trials with mesenchymal stem/ progenitor cells (MSCs) too far ahead of the science? Lessons from experimental hematology. Stem Cells *32*, 3055–3061.

Quante, M., Tu, S.P., Tomita, H., Gonda, T., Wang, S.S., Takashi, S., Baik, G.H., Shibata, W., Diprete, B., Betz, K.S., et al. (2011). Bone marrow-derived myofibroblasts contribute to the mesenchymal stem cell niche and promote tumor growth. Cancer Cell *19*, 257–272.

Rodriguez, R., Rubio, R., and Menendez, P. (2012). Modeling sarcomagenesis using multipotent mesenchymal stem cells. Cell Res. *22*, 62–77.

Seo, E., Basu-Roy, U., Gunaratne, P.H., Coarfa, C., Lim, D.S., Basilico, C., and Mansukhani, A. (2013). SOX2 regulates YAP1 to maintain stemness and determine cell fate in the osteo-adipo lineage. Cell Rep. *3*, 2075–2087.

Speight, P., Nakano, H., Kelley, T.J., Hinz, B., and Kapus, A. (2013). Differential topical susceptibility to TGFβ in intact and injured regions of the epithelium: key role in myofibroblast transition. Mol. Biol. Cell *24*, 3326–3336.

Swift, J., Ivanovska, I.L., Buxboim, A., Harada, T., Dingal, P.C., Pinter, J., Pajerowski, J.D., Spinler, K.R., Shin, J.W., Tewari, M., et al. (2013). Nuclear lamin-A scales with tissue stiffness and enhances matrix-directed differentiation. Science *341*, 1240104.

Tondeleir, D., Lambrechts, A., Müller, M., Jonckheere, V., Doll, T., Vandamme, D., Bakkali, K., Waterschoot, D., Lemaistre, M., Debeir, O., et al. (2012). Cells lacking β-actin are genetically reprogrammed and maintain conditional migratory capacity. Mol. Cell. Proteomics *11*, 255–271.

Tsai, C.C., Su, P.F., Huang, Y.F., Yew, T.L., and Hung, S.C. (2012). Oct4 and Nanog directly regulate Dnmt1 to maintain self-renewal and undifferentiated state in mesenchymal stem cells. Mol. Cell *47*, 169–182.

Varelas, X. (2014). The Hippo pathway effectors TAZ and YAP in development, homeostasis and disease. Development *141*, 1614–1626.

Varelas, X., Sakuma, R., Samavarchi-Tehrani, P., Peerani, R., Rao, B.M., Dembowy, J., Yaffe, M.B., Zandstra, P.W., and Wrana, J.L. (2008). TAZ controls Smad nucleocytoplasmic shuttling and regulates human embryonic stem-cell self-renewal. Nat. Cell Biol. *10*, 837–848.

Vermette, M., Trottier, V., Ménard, V., Saint-Pierre, L., Roy, A., and Fradette, J. (2007). Production of a new tissue-engineered adipose substitute from human adipose-derived stromal cells. Biomaterials *28*, 2850–2860.

Wada, K., Itoga, K., Okano, T., Yonemura, S., and Sasaki, H. (2011). Hippo pathway regulation by cell morphology and stress fibers. Development *138*, 3907–3914.

Wang, D., Park, J.S., Chu, J.S., Krakowski, A., Luo, K., Chen, D.J., and Li, S. (2004). Proteomic profiling of bone marrow mesenchymal stem cells upon transforming growth factor beta1 stimulation. J. Biol. Chem. *279*, 43725–43734.

Watabe, T., and Miyazono, K. (2009). Roles of TGF-beta family signaling in stem cell renewal and differentiation. Cell Res. *19*, 103–115.

Winer, J.P., Janmey, P.A., McCormick, M.E., and Funaki, M. (2009). Bone marrow-derived human mesenchymal stem cells become quiescent on soft substrates but remain responsive to chemical or mechanical stimuli. Tissue Eng. Part A *15*, 147–154.

Xiao, W., Mohseny, A.B., Hogendoorn, P., and Cleton-Jansen, A.-M. (2013). Mesenchymal stem cell transformation and sarcoma genesis. Clin. Sarcoma Res. *3*, 10. http://dx.doi.org/10.1186/2045-3329-3-10.

Yan, X., Liu, Y., Han, Q., Jia, M., Liao, L., Qi, M., and Zhao, R.C. (2007). Injured microenvironment directly guides the differentiation of engrafted Flk-1(+) mesenchymal stem cell in lung. Exp. Hematol. *35*, 1466–1475.

Yang, M.T., Fu, J., Wang, Y.K., Desai, R.A., and Chen, C.S. (2011). Assaying stem cell mechanobiology on microfabricated elastomeric

substrates with geometrically modulated rigidity. Nat. Protoc. *6*, 187–213.

Yang, C., Tibbitt, M.W., Basta, L., and Anseth, K.S. (2014). Mechanical memory and dosing influence stem cell fate. Nat. Mater. *13*, 645–652.

Yannarelli, G., Pacienza, N., Cuniberti, L., Medin, J., Davies, J., and Keating, A. (2013). Brief report: The potential role of epigenetics on multipotent cell differentiation capacity of mesenchymal stromal cells. Stem Cells *31*, 215–220.

Yu, F.X., Zhao, B., Panupinthu, N., Jewell, J.L., Lian, I., Wang, L.H., Zhao, J., Yuan, H., Tumaneng, K., Li, H., et al. (2012a). Regulation of the Hippo-YAP pathway by G-protein-coupled receptor signaling. Cell *150*, 780–791.

Yu, K.R., Yang, S.R., Jung, J.W., Kim, H., Ko, K., Han, D.W., Park, S.B., Choi, S.W., Kang, S.K., Schöler, H., and Kang, K.S. (2012b). CD49f enhances multipotency and maintains stemness through the direct regulation of OCT4 and SOX2. Stem Cells *30*, 876–887.